



HAL
open science

Differences between tree stem CO₂ efflux and O₂ influx rates cannot be explained by internal CO₂ transport or storage in large beech trees

Juliane Helm, Roberto L Salomón, Boaz Hilman, Jan Muhr, Alexander Knohl, Kathy Steppe, Yves Gibon, Cédric Cassan, Henrik Hartmann

► To cite this version:

Juliane Helm, Roberto L Salomón, Boaz Hilman, Jan Muhr, Alexander Knohl, et al.. Differences between tree stem CO₂ efflux and O₂ influx rates cannot be explained by internal CO₂ transport or storage in large beech trees. *Plant, Cell and Environment*, 2023, Online first, 10.1111/pce.14614 . hal-04121662

HAL Id: hal-04121662

<https://hal.inrae.fr/hal-04121662>

Submitted on 8 Jun 2023






HAL is a multi-disciplinary open access archive for the deposit and dissemination of scientific research documents, whether they are published or not. The documents may come from teaching and research institutions in France or abroad, or from public or private research centers.

L'archive ouverte pluridisciplinaire **HAL**, est destinée au dépôt et à la diffusion de documents scientifiques de niveau recherche, publiés ou non, émanant des établissements d'enseignement et de recherche français ou étrangers, des laboratoires publics ou privés.



Distributed under a Creative Commons Attribution 4.0 International License

Differences between tree stem CO₂ efflux and O₂ influx rates cannot be explained by internal CO₂ transport or storage in large beech trees

Juliane Helm^{1,2}  | Roberto L. Salomón^{3,4}  | Boaz Hilman¹  | Jan Muhr^{1,5,6} | Alexander Knohl⁶ | Kathy Steppe⁴  | Yves Gibon⁷ | Cédric Cassan⁷ | Henrik Hartmann^{1,8} 

¹Department of Biogeochemical Processes, Max-Planck-Institute for Biogeochemistry, Jena, Germany

²Department of Environmental Sciences–Botany, Basel University, Basel, Switzerland

³Department of Natural Systems and Resources, Technical University of Madrid (UPM), Madrid, Spain

⁴Department of Plants and Crops, Laboratory of Plant Ecology, Faculty of Bioscience Engineering, Ghent University, Ghent, Belgium

⁵Department of Forest Botany and Tree Physiology, Laboratory for Radioisotopes, Georg-August University Göttingen, Göttingen, Germany

⁶Department of Bioclimatology, Georg-August University Göttingen, Göttingen, Germany

⁷UMR 1332 Biologie du Fruit et Pathologie, INRAE, University of Bordeaux, Villenave d'Ornon, France

⁸Institute for Forest Protection, Julius Kühn-Institute, Federal Research Centre for Cultivated Plants, Quedlinburg, Germany

Correspondence

Juliane Helm, Max-Planck-Institute for Biogeochemistry, Biogeochemical Processes, Hans-Knöll-Str.10, 07743 Jena, Germany.
Email: jhelm@bgc-jena.mpg.de

Funding information

European Research Council under the European Union's Horizon 2020 research and innovation programme (grant agreement no. 682512 - OXYFLUX); Research Foundation Flanders (FWO) and the Marie Skłodowska-Curie research programme (665501)

Abstract

Tree stem respiration (R_S) is a substantial component of the forest carbon balance. The mass balance approach uses stem CO₂ efflux and internal xylem fluxes to sum up R_S , while the oxygen-based method assumes O₂ influx as a proxy of R_S . So far, both approaches have yielded inconsistent results regarding the fate of respired CO₂ in tree stems, a major challenge for quantifying forest carbon dynamics. We collected a data set of CO₂ efflux, O₂ influx, xylem CO₂ concentration, sap flow, sap pH, stem temperature, nonstructural carbohydrates concentration and potential phosphoenolpyruvate carboxylase (PEPC) capacity on mature beech trees to identify the sources of differences between approaches. The ratio of CO₂ efflux to O₂ influx was consistently below unity (0.7) along a 3-m vertical gradient, but internal fluxes did not bridge the gap between influx and efflux, nor did we find evidence for changes in respiratory substrate use. PEPC capacity was comparable with that previously reported in green current-year twigs. Although we could not reconcile differences between approaches, results shed light on the uncertain fate of CO₂ respired by parenchyma cells across the sapwood. Unexpected high values of PEPC

Abbreviations: ARD, apparent respiratory difference, as O₂ influx–CO₂ efflux; ARQ, apparent respiratory quotient, as CO₂ efflux/O₂ influx; [CO₂], [CO₂] in the gas phase; [CO₂*], dissolved inorganic carbon comprises of dissolved CO₂, carbonic acid (H₂CO₃), bicarbonate (HCO₃⁻) and carbonate (CO₃²⁻); E_{CO_2} , stem CO₂ efflux to the atmosphere (stem-surface); F_T , transport of dissolved respired C in the xylem sap; I_{O_2} , stem O₂ influx (stem-surface); PEPC, phosphoenolpyruvate carboxylase; enzyme for CO₂ fixation; R_S , stem respiration; ΔS , storage flux, as the temporal change in dissolved CO₂ in the sap.

This is an open access article under the terms of the Creative Commons Attribution License, which permits use, distribution and reproduction in any medium, provided the original work is properly cited.

© 2023 The Authors. *Plant, Cell & Environment* published by John Wiley & Sons Ltd.

capacity highlight its potential relevance as a mechanism of local CO₂ removal, which merits further research.

KEYWORDS

carbon dioxide transport, CO₂/O₂ ratio, mature trees, oxygen consumption, temperate forest, vertical stem gradient

1 | INTRODUCTION

Tree stem respiration (R_S) is an important component of the forest carbon (C) budget and is estimated to account for 5%–42% of total ecosystem respiration (Campioli et al., 2016; R. L. Salomón et al., 2017; Yang et al., 2016). Respiration rate is usually extrapolated to the whole stem from CO₂ efflux measurements at breast height. Even though direct measurements of CO₂ efflux are easy to conduct, various processes can decouple CO₂ efflux from R_S , resulting in mismatches of up to 45% (Hilman et al., 2019; R. Teskey & McGuire, 2007): (1) Dissolution of CO₂ in xylem water (Aubrey & Teskey, 2009; Bloemen et al., 2013; R. Teskey & McGuire, 2007), (2) axial CO₂ diffusivity (De Roo et al., 2019), (3) nonphotosynthetic CO₂ refixation via the enzymes carbonic anhydrase and phosphoenolpyruvate carboxylase (PEPC) (Berveiller & Damesin, 2008), or (4) photosynthetic CO₂ refixation via woody tissue photosynthesis (e.g., Ávila et al., 2014; De Roo et al., 2020; Pfanz et al., 2002; Steppe et al., 2015). Even if we could accurately estimate R_S at a given stem point, upscaling R_S to the whole tree level in mature stands is questionable as the relative contribution of the above-mentioned processes might vary with stem height (Ceschia et al., 2002).

Two main measurement approaches have been applied to estimate R_S . The carbon-based mass balance approach (McGuire & Teskey, 2004) not only considers CO₂ efflux (E_{CO_2}), but also takes into account the dissolution of CO₂ in the xylem (accounting for its equilibrium species H₂CO₃, HCO₃⁻ and CO₃²⁻; hereafter CO₂^{*}), its vertical transport through the xylem sap (F_T) and the CO₂ storage flux (ΔS), as the accumulation or depletion of CO₂ in the xylem sap over time, to achieve a more precise estimation of R_S on a volume basis ($\mu\text{mol m}^{-3} \text{s}^{-1}$):

$$R_S = E_{CO_2} + F_T + \Delta S. \quad (1)$$

Most studies applying the mass balance approach examined the contribution of CO₂ efflux, CO₂ transport and CO₂ storage to R_S in small trees or saplings (e.g., McGuire & Teskey, 2004; R. L. Salomón et al., 2018; Saveyn, Steppe, McGuire, et al., 2008) due to the easiness of constructing custom-made stem cuvettes surrounding the whole stem. However, applying findings from small trees to interpret CO₂ efflux in mature trees could be hampered by the long radial diffusive pathway in thick stems, which could result in significantly limited CO₂ diffusion rates (Steppe et al., 2007). This assumption is supported by findings in yellow poplar, where the relative

contribution of CO₂ efflux to R_S decreased with stem diameter (up to 60 cm), while CO₂ transport increased with stem size, as could be expected by larger sapwood conductive area, transpiration rates, and potential for CO₂ removal from the point of production (Fan et al., 2017).

Many studies have relied primarily on CO₂ efflux (and CO₂ transport) to estimate R_S ; nevertheless, aerobic respiration involves oxygen (O₂) consumption, and the influx of O₂ from the atmosphere into the stem (I_{O_2}) can also serve as a proxy for R_S . The second measurement approach to estimate R_S is based on simultaneous measurements of O₂ influx and CO₂ efflux. Given the much lower water solubility of O₂ compared with CO₂ (Dejours, 1981), dissolution effects and vertical transport should play a potentially negligible role for O₂. Boosted by technological improvements to register small O₂ fluctuations in an atmosphere with a large O₂ background, emerging interest arises in the coupled measurement of CO₂ efflux and O₂ influx at the stem surface (Angert & Sherer, 2011; Hilman & Angert, 2016). The ratio of CO₂ efflux to O₂ influx is called the respiratory quotient (RQ) at the cell level. The cell-level RQ allows exploring the substrate of respiratory metabolism. In trees, non-structural carbohydrates (NSC) are assumed to be the primary respiratory substrate, theoretically resulting in a RQ of ~1. More O₂ is needed for the breakdown of lipids compared with carbohydrates, resulting in RQ ~0.7 (Masiello et al., 2008). Organic acids catabolism would yield RQ above one because of the greater O₂ content of those molecules being oxidized (Masiello et al., 2008). At the organ level, as the stem in this case, the ratio of CO₂ efflux to O₂ influx at the surface is named the apparent respiratory quotient (ARQ) (Angert & Sherer, 2011):

$$ARQ = \frac{E_{CO_2}}{I_{O_2}}. \quad (2)$$

Therefore, simultaneous measurements of both gases allow for the assessment of potential shifts in respiratory substrate over time and under environmental stresses (Fischer et al., 2015). Furthermore, the ARQ can be affected by postrespiratory processes (Trumbore et al., 2013), providing information about the role of CO₂ dissolution and transport on R_S estimates, as CO₂ is highly soluble in xylem sap, while O₂ is less soluble. Hereby, assuming NSC as respiratory substrate, RQ would be ~1, and so would the ARQ as long as CO₂ transport and storage were negligible, as CO₂ efflux versus O₂ influx equalize. However, Hilman et al. (2019) showed the inability of sap flow (and hence CO₂ transport) to account for the variability in the ARQ of *Q. ilex* trees. Authors suggested CO₂ refixation via the

enzyme PEPC as the primary cause of ARQ below the unit, a mechanism of local CO₂ removal commonly overlooked in *R_s* research. However, the role of PEPC capacity in mature stems is still speculative as it has mainly been investigated in C4 plants and only in leaves and young green twigs of C3 plants (Berveiller & Damesin, 2008).

It is essential to reconcile insights gained through the mass balance approach and oxygen-based measurement methods, which disagree on the primary factor causing the mismatch between *R_s* and CO₂ efflux, either CO₂ transport through the xylem and storage or PEPC-mediated CO₂ fixation, respectively. Note that both approaches commonly use opaque stem cuvettes or chambers, precluding photosynthetic re-assimilation of locally respired CO₂ (see De Roo et al., 2020). Mathematically, as a first approximation assuming *R_s* and O₂ influx are equivalent, the mass balance could be formulated as follows:

$$ARD = I_{O_2} - E_{CO_2} = R_s - E_{CO_2} = F_T + \Delta S, \quad (3)$$

where the apparent respiratory difference (ARD), as an alternative metric to interpret the mismatch of CO₂ and O₂ fluxes in absolute terms, should equal the amount of locally respired CO₂ transported and stored if CO₂ re-fixation (either photosynthetic or nonphotosynthetic) is negligible. If the latter assumption is valid, carbon- and oxygen-based methods could be indistinguishably applied to estimate *R_s*. If not, it would be necessary to revisit underlying assumptions from both approaches to constrain the interpretation of each other and provide a more comprehensive perspective on the fate of respired CO₂ not emitted locally to the atmosphere. This is precisely the main challenge in research on the metabolism of woody tissue respiration. A direct comparison of both approaches is lacking so far. By combining both approaches with the same individuals and under the same conditions, it would be possible to assess whether discrepancies observed so far vanish or whether assumptions should be revisited.

To do so, we continuously monitored the vertical and temporal variability in CO₂ efflux, O₂ influx and xylem [CO₂] along a 3-m stem gradient in beech trees (*Fagus sylvatica* L.) during 1.5 summer months. Importantly, the study was performed in large mature trees, in which the contribution of CO₂ transport to *R_s* is expected to be higher (Fan et al., 2017), thereby enhancing the potential discrepancies between carbon- and oxygen-based approaches. Required additional variables to estimate the abovementioned respiration-related variables, like stem temperature, sap flow rate, and twig sap pH were also measured. Additionally, NSC concentrations and PEPC capacity from stem discs of the outermost tissues were discretely measured to evaluate potential shifts in substrate stoichiometry and the role of PEPC fixation on respiratory fluxes, respectively. We addressed the following hypothesis: When concurrently applying the carbon- and oxygen-based approaches in the same trees, xylem CO₂ transport and storage can close the gap between O₂ influx and CO₂ efflux fluxes (i.e., the ARD = 0). Alternatively, the fraction of missing CO₂ not explained by xylem CO₂ transport and storage could be attributed to CO₂ re-fixation via PEPC capacity if significant in large mature stems.

2 | MATERIALS AND METHODS

2.1 | Site description and experimental set-up

The experiment was conducted in a managed pure 130-year-old beech stand at ~100 m distance to the Fluxnet tower site Leinefelde (DE-Lnf, <https://doi.org/10.18140/FLX/1440150>) in the forest district of Heiligenstadt near the city of Leinefelde (51°20'N, 10°22'E; altitude 450 m a.s.l.; Thuringia; central Germany). The mean annual air temperature and precipitation are 8.3 ± 0.7°C and 601 ± 154 mm (Tamrakar et al., 2018). We measured four even-sized mature beech trees with a tree height of ca. 38 m and stem diameter at breast height (DBH) ranging between 0.38 and 0.54 m (Table 1) during July and August 2019 (Days of year [DOY] 185–226).

2.2 | Stem CO₂ efflux, O₂ influx and xylem [CO₂]

Stem CO₂ efflux and O₂ influx at the stem surface were measured hourly on every tree at three stem heights (1, 2.5, and 4 m) following the approach described in Helm et al. (2021). Briefly, we installed a custom-made chamber in each stem location that consisted of (i) a closed-porous cell foam and a base plate of 20 cm length, 10 cm width, and 4 cm height, (ii) a waterproof housing for the CO₂ and O₂ sensors with a removable lid for easy exchange of the sensors, and (iii) a transport-case containing an air pump, an Arduino® unit for data logging and 5 V power bank battery for power supply (800 mAh, Li-ion type, MP-50000; XTPower). See Supporting Information: Figures S1 and S2 for a schematic overview and a photograph of the set-up. Chambers were installed on the north side of the trees, and chambers were covered with aluminium foil to avoid direct solar radiation and impede local woody tissue photosynthesis. Chambers were attached against the tree stem using three ratchet straps. The measurement principle is based on a closed system with measurement cycles of 45 min followed by 15 min to flush the chamber's headspace with ambient air. To monitor [CO₂] increase and [O₂] decrease within the chamber headspace, a nondispersive infrared (NDIR) absorption sensor (COZIR; Gas Sensing Solution) and an optical fluorescence quenching sensor (LuminOx sealed, LOX-02-S; SST Sensing Ltd) were used, respectively. The relative humidity sensor integrated within the COZIR device accounted for the dilution effect of changing H₂O and CO₂ concentrations and correct O₂ measurements (for further details, see Helm et al., 2021). Sensors

TABLE 1 Diameter at breast height (DBH) and sapwood depth of the four beech trees.

Tree	Diameter (cm)	Sapwood depth (cm)
1	41	12.5
2	45	13.5
3	54	16.5
4	38	12.0

were changed after 3 weeks to limit reading drift (Helm et al., 2021). CO₂ efflux and O₂ influx on a surface basis (μmol m⁻² s⁻¹) were calculated from the linear CO₂ increase and O₂ decrease of the first 20-min time interval (of the 45 min measurement cycle excluding 3 min after flushing) following Equation (4):

$$E_{\text{CO}_2} \text{ or } I_{\text{O}_2} = \frac{\Delta C}{\Delta t} \times \frac{V}{A} \times \frac{P}{R \times T}, \quad (4)$$

where ΔC/Δt is the change in gas concentration over time (ppm s⁻¹) for CO₂ or O₂, V is the chamber headspace volume (m³) determined by water displacement, A is the stem surface area (m²), P is the barometric pressure (kPa), R is the molar gas constant (m³ kPa K⁻¹ mol⁻¹), and T is the temperature (K) obtained from the COZIR sensor. From CO₂ efflux and O₂ influx time series, the ARQ and ARD were calculated following Equation (2) and (3).

The concentration of xylem [CO₂] in the gas phase (%) was measured with NDIR CO₂ sensors (GMP221 and GMP251; Vaisala Inc.) calibrated before installation using reference gases at known [CO₂] of 0%, 5%, 10% and 15%. For each sensor, we drilled a 40 mm deep and 25 mm wide hole into the stem and pushed the probe (length: 96 mm) halfway within the hole (~20 mm), leaving a closed headspace in the xylem tissues beyond the cambium layer. Synthetic rubber sealant (Teroson RB IX; Henkel) was used for isolation from the atmospheric gas. Four sensors were installed in each tree along the vertical profile monitored with stem chambers at 1, 2.35, 2.65 and 4 m. We initially envisaged applying the mass balance approach in the 30-cm-length stem segment between 2.35 and 2.65 m probes. Nevertheless, we eventually decided to average the xylem [CO₂] time series from these two probes to survey longer (and more representative) stem segments, from 1 to 2.5 m (lower stem) and from 2.5 to 4 m (upper stem) (Supporting Information: Figure S1). Probes were placed ca. 10 cm from each chamber on the northwest side of the trees. Readings of the 16 sensors were recorded every 5 min with a datalogger (CR1000x; Campbell Scientific) for the whole experiment period.

2.3 | Xylem CO₂ transport and storage

The amount of CO₂ transported upwards through the xylem and stored within the xylem was estimated in the lower and upper stem segments. The concentration of dissolved CO₂ in xylem sap ([CO₂*], mol CO₂ l⁻¹) was calculated using temperature-dependent Henry's Law coefficients (Levy et al., 1999; McGuire & Teskey, 2002), assuming equilibrium between CO₂ in the gaseous and liquid phases. For this, xylem [CO₂] in the gas phase, xylem sap pH, and stem temperature must be known. To monitor sap pH, xylem sap was collected from twigs of low branches of monitored trees (n = 3, as one tree was inaccessible for sampling) using a Scholander pressure chamber at four sampling dates (DOYs 204, 212, 218 and 226). Sap samples were quickly placed in Eppendorf tubes and a cold box for transportation to the laboratory and then stored in a refrigerator until measurement. Xylem sap pH was measured using a pH meter (Five

Easy; Mettler Toledo) with a microelectrode (InLab[®], Ultra-Micro-ISM; Mettler Toledo). Preliminary tests confirmed that sap pH did not significantly vary over the sample storage period. Stem temperature (T_{stem}, °C) was continuously measured and recorded with a datalogger (CR1000x; Campbell Scientific) every 5 min using thermocouples inserted at 2 cm depth next to each stem chamber.

Once sap [CO₂*] was known, CO₂ transport (F_T, μmol CO₂ m⁻³ s⁻¹) for both lower and upper stem segments were estimated according to:

$$F_T = \left(\frac{SF}{v} \right) \times \Delta[\text{CO}_2^*], \quad (5)$$

where SF is the sap flow rate (l s⁻¹), v is the sapwood volume (m³), and Δ[CO₂*] is the difference in sap [CO₂*] above and below the corresponding stem segment (μmol l⁻¹). The sap flow rate was estimated as the product of sap flux density (l cm⁻² h⁻¹) and sapwood area (cm⁻²) using the Sap Flow Tool software (Plant AnalytiX). Sap flux density was monitored using sap flow meters SFM1 (ICT International Pty Ltd.) operated by the heat ratio method (Burgess et al., 2001), assuming a stem water content of 400 l m⁻³ (Gartner et al., 2004). Sap flow probes were installed at breast height on the north side of the trees, and measurements were recorded every 15 min.

A staining method was applied to determine the sapwood area; upon extraction of one wood core per tree at breast height on the northwest side of the tree (until the pith), a blue dye (E131) was injected into the hole, and a second core was extracted one cm above the first one after 1 h. Sapwood depth was determined by the length of the stained region of the core and assuming a cylindrical shape for both heartwood and sapwood (Table 1) (Goldstein et al., 1998).

The stem CO₂ storage flux (ΔS) was estimated as a function of the time derivative of [CO₂*] in the xylem; that is, the rate of accumulation and depletion of dissolved CO₂ for both lower and upper stem segments according to:

$$\Delta S = \frac{d[\text{CO}_2^*]}{dt} \times \text{WC}. \quad (6)$$

2.4 | Soil water content and shoot water potential

Soil water content (%) was continuously measured at the meteorological flux tower with one sensor (ML-2x; DeltaT) inserted at 16 cm depth, 100 m away from our instrumented trees, with a temporal resolution of 10 min. Shoot water potential (MPa) was measured around solar midday (as for sap pH sampling) at four sampling dates (DOYs 204, 212, 218, and 226) using the Scholander pressure chamber.

2.5 | PEPC capacity and NSC in woody tissues

We took one stem disc (one cm-length, bark to xylem) at three stem heights (1, 2.5, and 4 m) on the south side of each monitored tree on 14 August (DOY 226). Samples were immediately frozen in liquid

nitrogen to stop the metabolic activity and transported to the laboratory. Stem discs were stored at -80°C before grinding into a fine powder in liquid nitrogen with a mortar and pestle. 20 mg of woody tissue material was used for the discontinuous assay performed in a 96-well microplate (Bénard & Gibon, 2016). Briefly, aliquots were extracted by shaking with an extraction buffer. After centrifugation (7 min, 3000 g, 4°C), extracts were diluted and incubated for 20 min. The reaction was stopped with HCl. The sealed microplate was then incubated at 95°C for 10 min to destroy NADH. After cooling down, each well was neutralised with NaOH and Tricine-KOH pH 9.0 to adjust the pH to 9.0. The absorbance was read at 570 nm (30°C) until rates were stabilised. Reaction rates (mOD min^{-1}) were used to calculate the amount of NAD⁺ formed during the first step of the assay. All pipetting steps were performed using a 96-head robot (Hamilton Star), and absorbances were measured in a filter-based microplate reader (SAFAS MP96). For further details, see Supporting Information: Methods S1 and Bénard and Gibon (2016).

We measured soluble sugars and starch in stem cores from the instrumented trees following the Landhausser et al. (2018) protocol. One stem core per height (1, 2.5, 4 m, south-side) was collected on 4 July (DOY 185) and 14 August (DOY 226) for NSC measurements. Samples were stored in cooling bags for transportation and then oven-dried at 60°C for 72 h. Stem cores were cut into two 2-cm long sections starting at the cambium (wood depth: 0–2 cm and 2–4 cm) and ground into a fine powder (ball mill, MM 400; Retsch). We extracted the soluble sugars glucose, fructose, sucrose, and starch from each sample. Briefly, ~ 30 mg of dry plant powder was extracted with 80% ethanol. Supernatants were analysed by High-Performance Liquid Chromatography coupled to a Pulsed Amperometric Detection (HPLC-PAD) for soluble sugar determination. We enzymatically converted the starch from the remaining pellet to glucose using α -amylase amyloglucosidase. Glucose hydrolysate was measured by the HPLC.

2.6 | Data analysis

Statistical analyses were performed using R software (R Development Core Team, 2019). CO₂ efflux and O₂ influx data were discarded when the R² of the linear fit for CO₂ and O₂ readings were below 0.96 to ensure good data quality. For gap filling, we used the *pad* function in *padr* package. To test whether the average daily values of CO₂ efflux, O₂ influx and xylem [CO₂] varied with stem height, linear mixed models were adjusted using the *lme* function in *nlme* package (Pinheiro et al., 2017), considering height as a fixed factor and tree as a random factor including an autocorrelation structure to account for repeated measurements. To test whether PEPC capacity varied with stem height, and sap pH among sampling dates, linear mixed models were adjusted likewise, considering the tree as a random factor. The normality of residuals was checked visually. When significant, differences among heights were tested post hoc with Tukey contrasts using the *emmeans* function (*emmeans* package). Consistency between carbon- and oxygen-based measurements was tested by

evaluating the relationship between R_s ($E_{\text{CO}_2} + F_T + \Delta S$) and O₂ influx, and between CO₂ internal fluxes ($F_T + \Delta S$) and ARD, with mixed models considering tree a random factor. Potential deviances from the 1:1 relationship would indicate a lack of consistency between methodological approaches, hence the need to revisit the underlying assumptions of Equation (3). The conditional and marginal R² (Nakagawa & Schielzeth, 2013) of these models was estimated using *r2_nakagawa* function (*performance* package) to further evaluate the degree of agreement between approaches. Finally, sap flow, sap [CO₂*] and the ARD were normalized to their daily maxima, and subdaily patterns were compared to evaluate the potential of xylem transport to remove locally respired CO₂ on a subdaily basis.

3 | RESULTS

3.1 | Stem temperature, soil water content, sap flow rate and shoot water potential

The mean stem temperature during the experiment was 17.7°C , with minimum values of 10°C during early July and peaking at the end of July with values close to 30°C (Figure 1a). Volumetric soil water content at 16 cm depth was lowest end of July, reaching minimum values of 15.7 vol% and maximum values of 19.0 vol% afterwards following summer rains (Figure 1b). Sap flow rate showed a typical subdaily pattern with maximum rates of 30 l h^{-1} during sunny and warm days (Figure 1c). Shoot midday Ψ (shoot water potential) was close to -1.4 MPa on most measurement days, except the one following rains when it relaxed up to -0.5 MPa (Figure 1c).

3.2 | Gas exchange and internal [CO₂] at different stem heights

The vertical position did not affect CO₂ efflux and O₂ influx ($p = 0.69$ and 0.71 , respectively). Mean daily CO₂ efflux ($\pm \text{SE}$) was 2.9 ± 0.6 , 2.7 ± 0.4 and $2.3 \pm 0.6 \mu\text{mol m}^{-2} \text{ s}^{-1}$ at 1, 2.5, and 4 m stem height, respectively (Figure 2a). Mean daily O₂ influx was 4.1 ± 0.7 , 3.9 ± 0.5 and $3.3 \pm 0.6 \mu\text{mol m}^{-2} \text{ s}^{-1}$, respectively (Figure 2b). O₂ influx was consistently higher than CO₂ efflux along the vertical gradient ($p < 0.001$), resulting in mean daily ARQ of 0.71 ± 0.04 , 0.69 ± 0.04 and 0.69 ± 0.06 at 1, 2.5 and 4 m stem height, respectively (Figure 2c). Xylem [CO₂] ranged from ca. 5.9% to 12.4%, with no significant effect of height over the whole surveyed period (Figure 2d; $p = 0.11$). However, when considering the last third of the experiment (1–14 August), stem height did affect xylem [CO₂] ($p = 0.03$), with values being lower at 1 m compared with 2.5 m height. Sap pH ranged between 6.48 and 7.41 over the measurement period (Figure 2d), and differences in sap pH among trees ($p = 0.17$) or dates ($p = 0.21$) were not significant. Stem temperature had a strong effect on xylem [CO₂] ($p < 0.001$), CO₂ efflux and O₂ influx ($p < 0.01$). Likewise, respiratory fluxes had maximum values during the afternoon, following subdaily thermal dynamics.

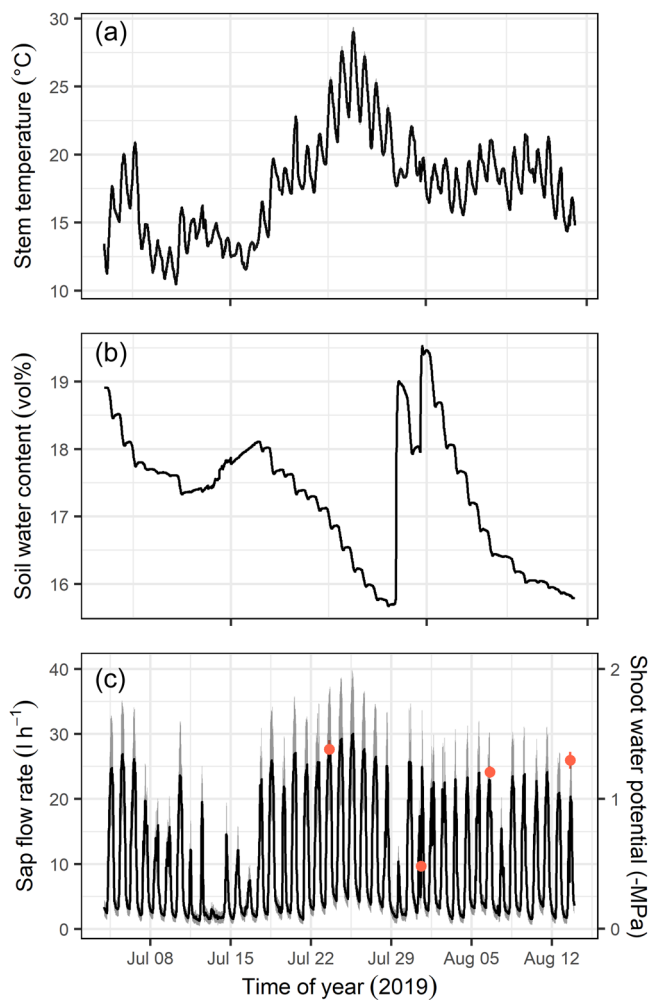


FIGURE 1 (a) One-hour average of stem temperature, (b) volumetric soil water content, and (c) sap flow rate (lines) with shoot water potential (orange dots) from 4 July to 14 August 2019. Shading in (c) indicates average ± 1 SE across the beech trees ($n = 4$). [Color figure can be viewed at wileyonlinelibrary.com]

3.3 | PEPC capacity and NSC at different stem heights

Stem height had no significant effect on PEPC capacity in the outermost stem section ($p = 0.23$) and did not differ among trees ($p = 0.93$). Mean PEPC capacity was 760.5 ± 201.6 , 661.25 ± 60.2 and 547.25 ± 77.4 $\text{nmol min}^{-1} \text{gFW}^{-1}$ at 1, 2.5 and 4 m, respectively.

Stem height did not affect soluble sugar and starch concentrations ($p = 0.37$ and 0.40 , respectively) (Figure 3). Sapwood depth did affect NSC; both soluble sugar and starch concentrations were higher near the cambium (0–2 cm) than deeper into the sapwood (2–4 cm) ($p < 0.05$). Soluble sugar and starch concentrations were higher on the second sampling date in August (DOY 226) for the 0–2 cm depth ($p < 0.001$, $p < 0.01$ for soluble sugar and starch, respectively), while they remained constant deeper into the cambium ($p = 0.1$, $p = 0.6$ for soluble sugar and starch, respectively).

3.4 | Comparison of carbon- and oxygen-based estimates of R_S

We applied the mass balance approach on the lower (1–2.5 m) and upper (2.5–4 m) stem segments to estimate R_S and its contributors for comparison with the oxygen-based approach (Figure 4). In the lower stem segment, there was a positive vertical gradient in sap [CO_2^*], and CO_2 transport was, therefore, positive. Averaged across days and trees, the contribution of CO_2 efflux to R_S was $64.6 \pm 14.5\%$, and the remaining fraction was attributed to CO_2 transport ($35.8 \pm 14.3\%$), as CO_2 storage was negligible ($-0.4 \pm 0.2\%$). The R_S daily average (as the sum of E_{CO_2} , F_T and ΔS) was greater than O_2 influx, but on a subdaily basis, R_S exceeded O_2 influx only during the daytime. During night-time, R_S equalled CO_2 efflux, and both were lower than O_2 influx.

The upper stem showed a different pattern where the vertical gradient in sap [CO_2^*] approached zero and even became negative for the last 2 weeks of our study. As a consequence, the relative contributions of CO_2 transport ($-1.2 \pm 2.2\%$) and CO_2 storage ($0.0 \pm 2.2\%$) to R_S were negligible, and apparently, all the respired CO_2 diffused to the atmosphere ($E_{\text{CO}_2} = 101.1 \pm 22.9\%$). In this stem section, both CO_2 efflux and R_S were on average lower than O_2 influx for most of the surveyed period. Notably, the shift from positive towards negative CO_2 transport flux followed the peak in temperature and transpiration at the end of July.

Daily values of stem CO_2 efflux and O_2 influx showed good agreement (Figure 5a) with a slope of 0.65 ± 0.02 ($p < 0.0001$), a significant intercept of 0.23 ± 0.11 ($p < 0.05$), and conditional and marginal R^2 of 0.87 and 0.86, respectively. When this relation was forced through the origin (the intercept is zero), the slope increased to 0.69 ± 0.02 , which is in better agreement with the mean ARQ of 0.70. Nevertheless, carbon- and oxygen-based estimates of R_S showed poor consistency. Although R_S and O_2 influx were positively related (Figure 5b), the deviation of the mean slope from unity was significant (1.57 ± 0.18 ; $p < 0.0001$), as well as its intercept (-2.08 ± 1.01 ; $p < 0.05$). The model conditional and marginal R^2 were 0.52 and 0.31, respectively. The slope of the relation between the ARD and CO_2 internal fluxes ($F_T + \Delta S$) (Figure 5c) was almost 0 (0.056 ± 0.012 ; $p < 0.0001$), and its intercept was again significant (0.84 ± 0.09 ; $p < 0.0001$), denoting the limited potential of CO_2 transport and storage to bridge the gap between CO_2 efflux and O_2 influx. The conditional and marginal R^2 of this model were 0.21 and 0.13, respectively. Stem location did not affect the intercept of any of these relations ($p > 0.1$), according to the lack of consistency in vertical gradients of respiratory-related variables.

To further evaluate the potential of the transpiration stream to transport respired CO_2 away from its point of production, we evaluate the subdaily patterns of ARD, sap flow and sap [CO_2^*] (as a proxy of CO_2 solubility). For the comparison, we normalized the values of each variable to their corresponding daily maxima (Figure 6). Compared with sap flow dynamics, the ARD showed a relatively stable pattern over the 24-h period. It was higher during the daytime, with night-time reductions of ca. 30%–35% relative to the daily

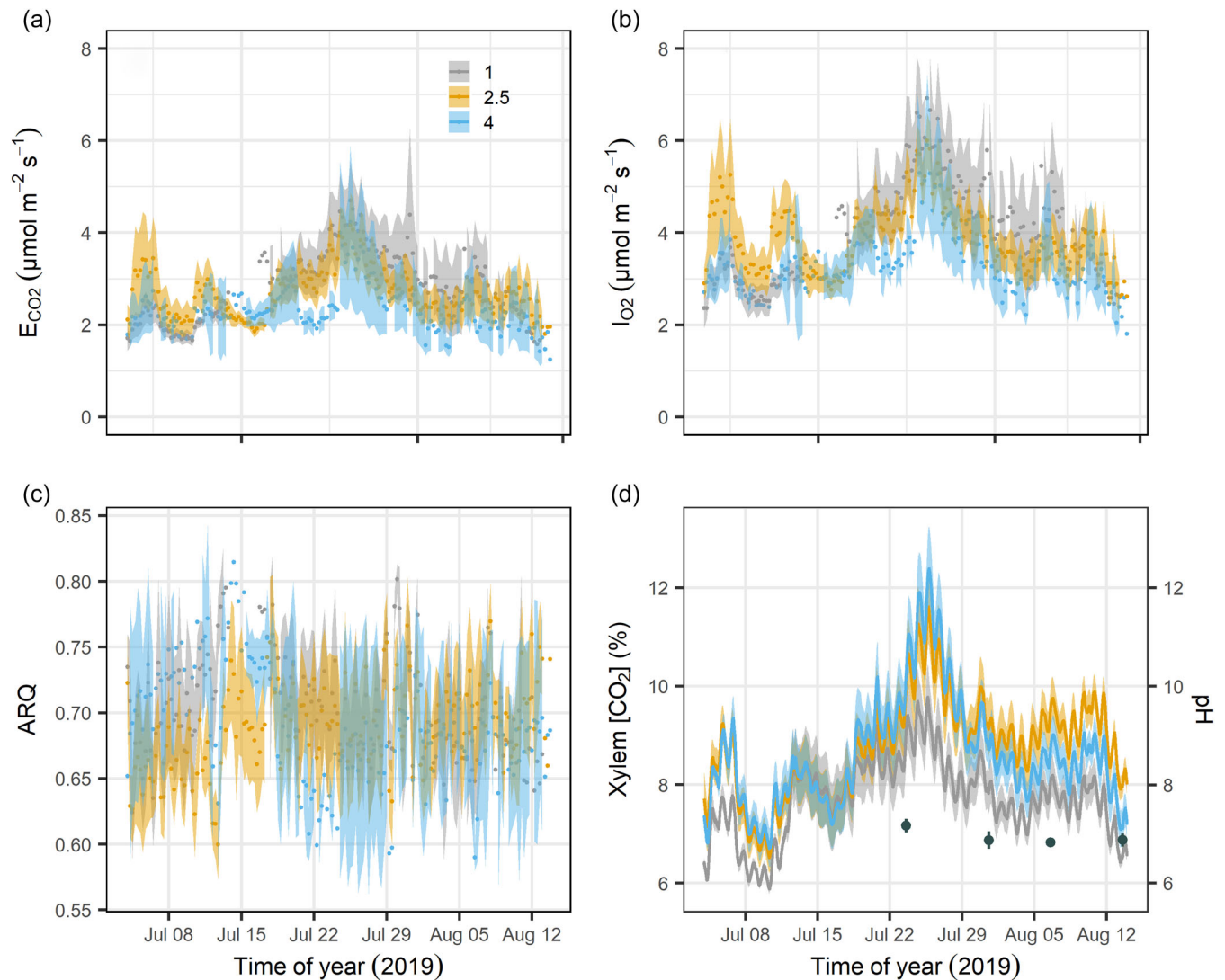


FIGURE 2 (a) CO₂ efflux (E_{CO_2}), (b) O₂ influx (I_{O_2}), (c) the apparent respiratory quotient (ARQ; E_{CO_2}/I_{O_2}) and (d) internal xylem [CO₂] at 1, 2.5 and 4 m height from 4 July to 14 August 2019. Sap pH (d, black dots) was measured from twigs ($n = 3$). [Color figure can be viewed at [wileyonlinelibrary.com](https://onlinelibrary.wiley.com/doi/10.1111/pce.14614)]

maxima. By contrast, sap flow showed night-time reductions of ca. 85%–90% relative to the daily maxima, denoting subdaily decoupling between CO₂ transport and the ARQ. Subdaily variation in sap [CO₂*] was minimal, with the highest values observed during night-time and limited reductions during daytime (<2%) according to the inverse relation between solubility and temperature.

4 | DISCUSSION

We combined a carbon-based mass balance approach and an oxygen-based method to estimate R_s and reconcile apparent discrepancies regarding the fate of respired CO₂ not locally emitted to the atmosphere. O₂ influx was consistently higher than CO₂ efflux across trees, locations and time, with ARQ fluctuating around 0.7 (Figures 2c and 5a), as similarly observed in several species applying the same

methodological approach (Angert et al., 2012; Hilman & Angert, 2016; Hilman et al., 2019). Assuming the beech trees use carbohydrates for respiration, the measured ARQ suggests that 30% of the respired CO₂ is retained in the stem. Figure 7 summarises potential sources of discrepancy between CO₂ efflux and O₂ influx. The ARQ could be attributed to an underestimation of the respiratory activity by CO₂ efflux measurements, an overestimation by O₂ influx, or a combination of both. In any case, we must be cautious about the specific methodological issues related to the measurement of the numerous variables monitored here (i.e., CO₂ efflux, O₂ influx, xylem [CO₂], sap flow, and sap pH), which might affect the magnitude of the mismatch between measurement approaches (see below).

No apparent vertical patterns in stem CO₂ efflux, O₂ influx and xylem [CO₂] were observed along a 3-m-long stem segment (Figure 2), likely because of the modest vertical gradient in 38-m-tall beech trees. The temporal variability of CO₂ efflux, O₂ influx and

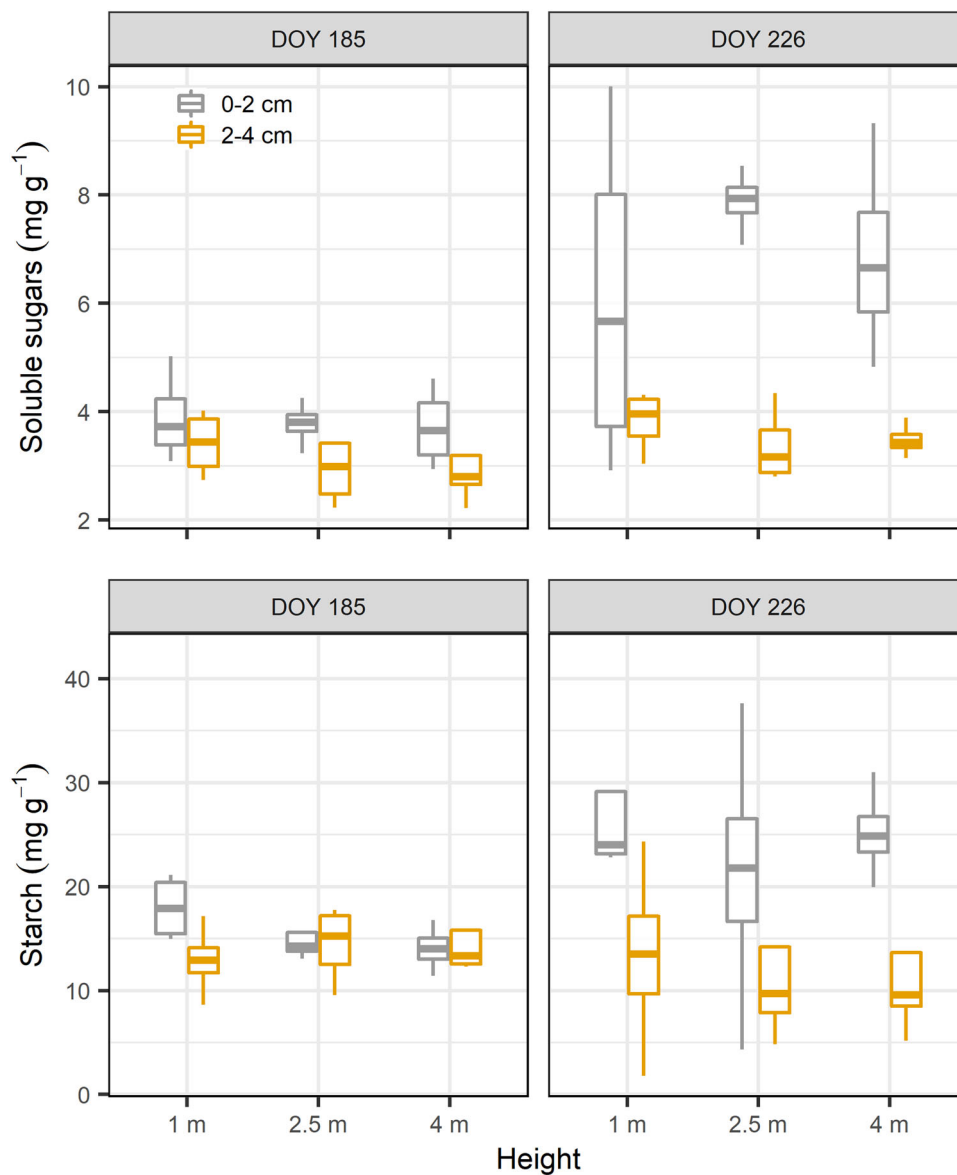


FIGURE 3 Starch and soluble sugar concentration (mg g DW^{-1}) in stem xylem tissues of beech trees at three stem heights, two wood depths, and two sampling dates ($n = 4$). Box whisker plots present the median, lower (25th), and upper (75th) percentiles, minimum and maximum values. Colours denote different sapwood depths. [Color figure can be viewed at wileyonlinelibrary.com]

xylem $[\text{CO}_2]$ showed that temperature was the dominant environmental driver controlling R_s , as similarly observed before (e.g., Acosta et al., 2008; Lavigne et al., 1996; Maier et al., 2010; Rodríguez-Calcerrada et al., 2014; Ryan et al., 1995). Interestingly, during and after the peak in temperature and respiratory fluxes at the end of July, xylem $[\text{CO}_2]$ did increase along the lower stem segment (from 1 to 2.5 m height) but remained relatively stable along the upper stem (from 2.5 to 4 m height). This observed difference in the vertical gradient of the xylem $[\text{CO}_2]$ led to contrasting contributions of CO_2 transport to R_s in the lower and upper stem segments, as discussed below. The lack of a significant relation of both CO_2 efflux and O_2 influx with soil water content denotes that the mild drought did not limit respiratory metabolism to a large extent. Interestingly, ARQ remained relatively stable over the 1.5 summer months, where a

temperature peak (30°C) occurred, suggesting similar sensitivity to temperature of CO_2 efflux and O_2 influx.

4.1 | CO_2 internal fluxes cannot explain the differences between stem O_2 influx and CO_2 efflux

Higher O_2 influx than CO_2 efflux could result from the higher solubility of CO_2 in xylem sap (30 fold) compared with O_2 (Dejours, 1981), hence the possibility of CO_2 dissolving in the sap solution and being transported upwards or stored. If true, this would be evident in our mature beech trees, whose large sapwood conducting area provides room for potentially high transport and storage of respired CO_2 (Fan et al., 2017). We found a

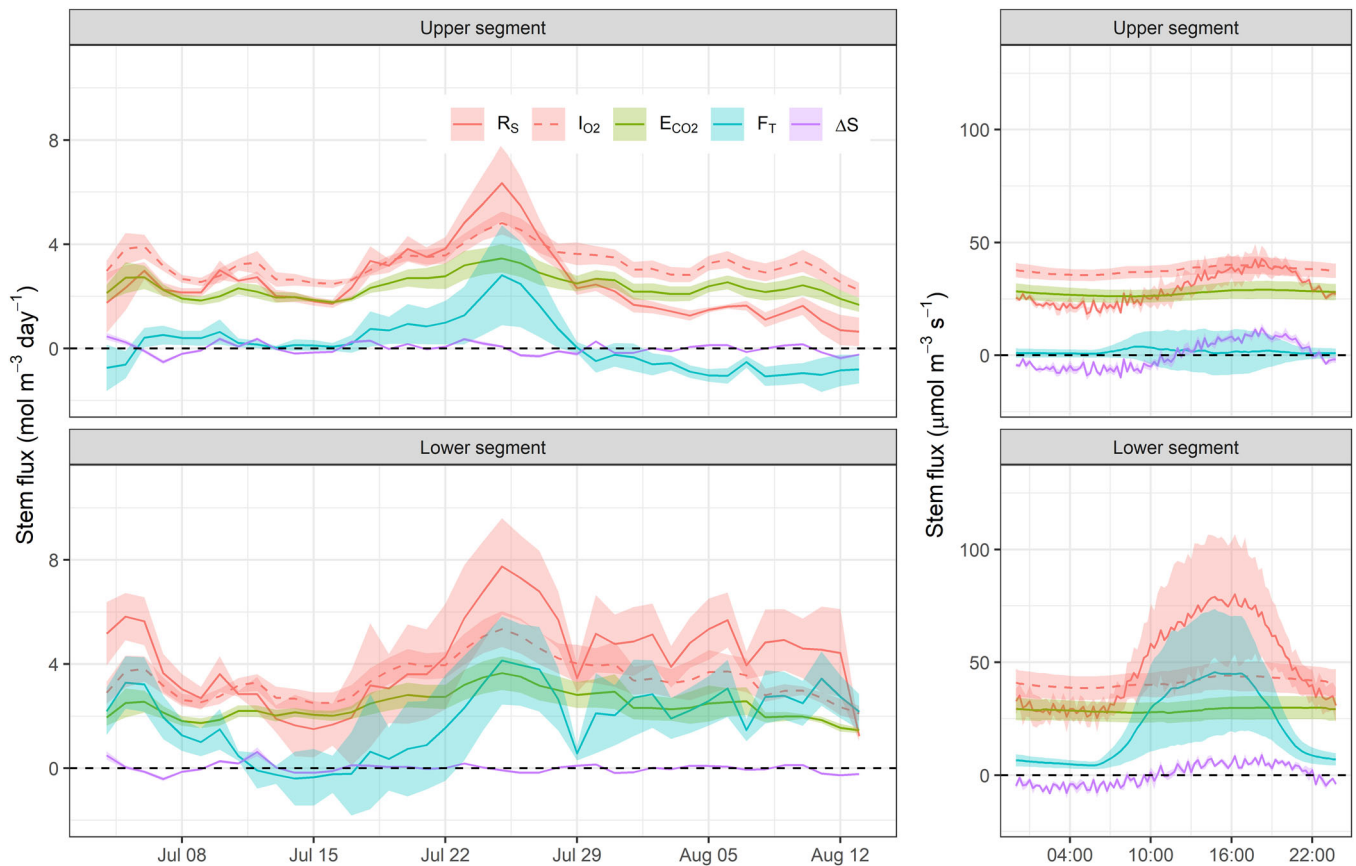


FIGURE 4 Seasonal (left-hand-side panels) and subdaily (right-hand-side panels) variation in carbon- and oxygen-based estimates of stem respiration (R_S and O_2 influx [I_{O_2}], respectively) in the lower (from 1 to 2.5 m) and upper (from 2.5 to 4 m) stem segments of four mature beech trees. Carbon-based R_S is calculated as the sum of CO_2 efflux to the atmosphere (E_{CO_2}), CO_2 transport through the xylem (F_T) and CO_2 storage (ΔS). Mean values \pm SE are shown with continuous lines and shaded areas. [Color figure can be viewed at [wileyonlinelibrary.com](https://onlinelibrary.wiley.com/doi/10.1111/pce.14614)]

nonnegligible contribution of CO_2 transport to R_S , up to 1/3 in the lower stem segment, highlighting the potentially significant role of CO_2 xylem transport in diverting root-respired CO_2 from soil measurements (Aubrey & Teskey, 2021). Nevertheless, we found two lines of evidence refuting our hypothesis, as CO_2 internal fluxes could not bridge the gap between stem O_2 influx and CO_2 efflux. First, the relation between O_2 influx and R_S diverged from the 1:1 line (Figure 5b), as indicated by a slope different from the unit and a significant intercept. Furthermore, the marginal $R^2 = 0.31$ of this relation denotes that stem O_2 influx accounted for less than one-third of the variability in the carbon-based estimate of R_S . Identical reasoning applies to the comparison between CO_2 internal fluxes ($F_T + \Delta S$) and ARD (Figure 5c), with a marginal R^2 of 0.13, further supporting the limited potential of xylem CO_2 transport and storage to predict the ARD. Second, if the ARD could be primarily ascribed to xylem CO_2 transport, ARD and sap flow subdaily variability should follow similar patterns (Bowman et al., 2005; McGuire & Teskey, 2004; McGuire et al., 2007). However, the subdaily variation in ARD was limited compared with sap flow (Figure 6). Specifically, ARD maintained values above 50% of the daily maxima during nighttime, when sap flow was reduced to a much larger extent, down to 10%–15% of the daily maxima. Moreover, sap $[CO_2^*]$ on a subdaily

basis was remarkably stable, with minimal reductions during daytime ascribed to temperature-driven reductions in CO_2 solubility, partly offset by the daytime increase in respiratory activity and xylem $[CO_2]$. Therefore, CO_2 solubility in sap could not significantly affect the strength of CO_2 transport as a mechanism to remove respired CO_2 from its production site. Taken together, subdaily patterns of ARD, sap flow and sap $[CO_2^*]$ thus provide further evidence of the limited role of the transpiration stream in filling the gap between CO_2 efflux and O_2 influx in this study. This observation agrees with Hilman et al. (2019), showing the inability of sap flow to account for the variability in ARD of *Q. ilex* trees.

Nevertheless, we must be cautious about the specific methodological issues related to the measurement of sap flow and sap pH and their corresponding propagation errors. For instance, sap flow measured with the heat pulse method often underestimates the actual sap flow, on average, by 35% (Steppe et al., 2010). Considering a proportional underestimation of CO_2 transport, its contribution to R_S would also increase in parallel, affecting the difference between R_S and O_2 influx differently among individuals and heights. Sap pH, especially above 6.5, is another critical factor for calculating CO_2 transport, as the solubility of CO_2 increases exponentially with pH. Here, we applied a constant pH value across daily and subdaily

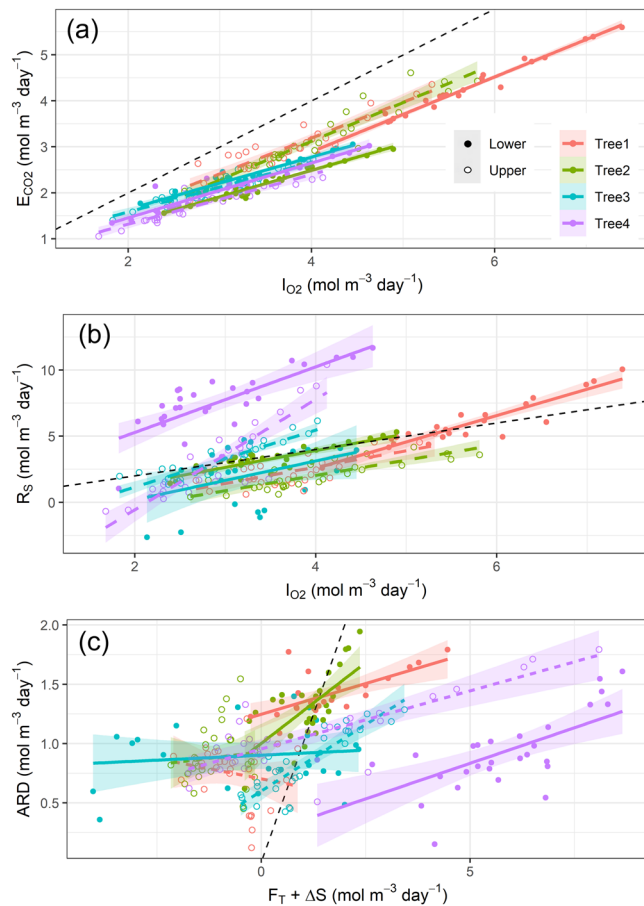


FIGURE 5 (a) Relationship between daily stem CO₂ efflux (E_{CO_2}) and O₂ influx (I_{O_2}) denoting apparent respiratory quotients below the unit. (b) The relationship between carbon-based estimates of stem respiration (R_S) and O₂ influx illustrates the deviation from the 1:1 line and, thus, discrepancies between measurement approaches. (c) The relationship between the apparent respiratory difference (ARD) and internal CO₂ transport and storage ($F_T + \Delta S$) indicates the limited potential of internal CO₂ transport and storage to predict the difference between CO₂ efflux and O₂ influx. Measurements were performed in four mature beech trees (shown by different colours) in the lower (from 1 to 2.5 m) and upper (from 2.5 to 4 m) stem segments (shown by different point and line types). Dashed black lines show the 1:1 relation. [Color figure can be viewed at [wileyonlinelibrary.com](https://onlinelibrary.wiley.com/doi/10.1111/pce.14614)]

temporal scales and assumed similar pH between twig sap and stem sap. However, these assumptions can lead to further CO₂ transport misestimation (Aubrey et al., 2011; Erda et al., 2014; R. Salomón et al., 2016) and deviances between carbon-based estimates of R_S and O₂ influx. Moreover, if parenchyma cells were damaged upon sap extraction, the sample might be contaminated, resulting in an overestimation of the pH values (Tarvainen et al., 2023) and hence CO₂ transport. Another source of uncertainty in ARQ estimation is the relative humidity correction applied to estimate O₂ influx. The relative humidity sensor integrated into the [CO₂] sensor has a slow response time, as shown in Helm et al. (2021). Assuming an underestimation of humidity levels in the measurement chamber

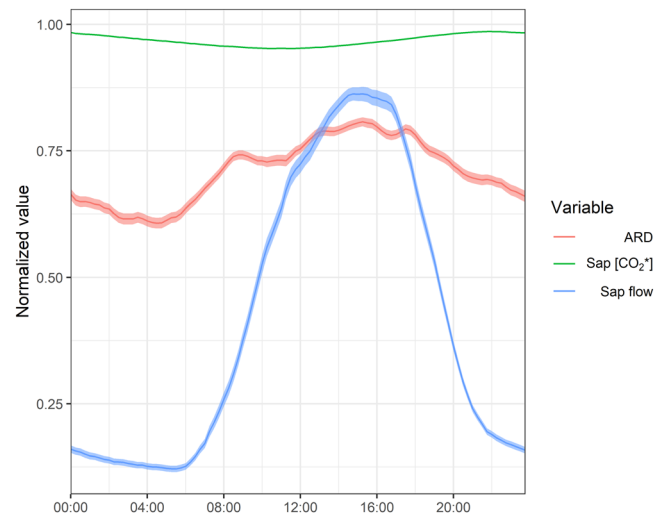


FIGURE 6 Subdaily variation in normalized values to the daily maxima of the apparent respiratory difference (ARD, as the difference between stem O₂ influx and CO₂ efflux), sap flow, and sap [CO₂] in the liquid phase ([CO₂*]). The night-time reduction in ARD was limited compared with that of sap flow, indicating a limited role of the transpiration stream in filling the gap between CO₂ efflux and O₂ influx. Subdaily patterns were averaged across four beech trees and two stem locations (lower and upper) over the experimental period. [Color figure can be viewed at [wileyonlinelibrary.com](https://onlinelibrary.wiley.com/doi/10.1111/pce.14614)]

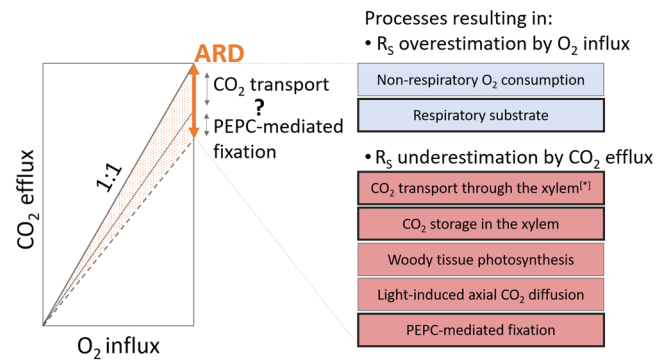


FIGURE 7 Overview of the potential factors contributing to the apparent respiratory difference (ARD), here observed as the difference between stem CO₂ efflux (E_{CO_2}) and O₂ influx (I_{O_2}) measurements (cf. Figure 5a). Our results suggest that CO₂ transport and PEPC-mediated fixation of CO₂ may be the main causes for the deviance from the 1:1 line. Nonrespiratory consumption of O₂ and respiratory substrate change can lead to overestimating stem respiration (R_S) by O₂ influx measurements. By contrast, R_S underestimation by CO₂ efflux measurements can be driven by CO₂ transport through the xylem (although, if coming from below, it can also lead to R_S overestimation^[*]), CO₂ storage in xylem sap, woody tissue photosynthesis (here avoided by using opaque stem chambers), light-induced axial CO₂ diffusion above or below the stem chamber, and PEPC-mediated fixation. Investigated processes within this study are shown with a black frame. [Color figure can be viewed at [wileyonlinelibrary.com](https://onlinelibrary.wiley.com/doi/10.1111/pce.14614)]

by, for example, 5%, the dilution correction required for O₂ estimation would increase the ARQ by ~0.001.

Regardless of these potential measurement uncertainties, we did not succeed in reconciling differences between the two approaches, which highlights a crucial methodological difference. The carbon-based approach estimates R_S based on fluxes measured at the stem surface and internal fluxes measured in the xylem, while the oxygen-based approach relies on O₂ influx at the stem surface. Therefore, the disagreement between approaches might be related to the fact that (i) CO₂ efflux and O₂ influx likely reflect respiration in the outermost tissues of the stem (bark, phloem, cambium and outer xylem) and that (ii) respiration of the inner sapwood in large trees cannot be appropriately detected by measurements taken at the surface. According to Fick's law of diffusion, the rate of gas (CO₂ or O₂) diffusion is inversely related to the length of the diffusive pathway (Nobel, 2009) and, therefore, such decoupling likely increases in large-sized trees. Here, in the mature beech trees with a sapwood depth between 12 and 16.5 cm, the diffusion of respired CO₂ by inner living cells is much lower than in seedlings and saplings, wherein each respiring cell is located nearer to the bark-atmosphere interface. Decoupling between internal respiratory fluxes and fluxes from the stem surface can be exacerbated by the high water content of the cambium layer (De Schepper et al., 2012), acting as a major diffusion barrier according to the slow gas diffusivity in water (ca. 10⁴ times lower than in air; Nobel 2009).

4.2 | PEPC-mediated CO₂ fixation as a relevant driver of the systematic mismatch between CO₂ efflux and O₂ influx

Higher O₂ influx than CO₂ efflux could be explained by CO₂ refixation via PEPC, which hinders CO₂ from being locally emitted. We measured PEPC capacity of 656 nmol min⁻¹ g FW⁻¹, equivalent to 22 nmol s⁻¹ g DW⁻¹ (assuming stem water content of 50%). For comparison, the PEPC capacity in current-year twigs of beech trees was 13 nmol s⁻¹ g DW⁻¹ (Hilman et al., 2019, recalculated from Berveiller & Damesin 2008), and 17 nmol s⁻¹ g DW⁻¹ in *Pinus sylvestris* (Hilman et al., 2019, recalculated from Ivanov et al., 2006). Therefore, the capacity of CO₂ refixation via PEPC measured here was comparable with that observed in younger, greener twigs.

In nonphotosynthetic tissues, PEPC is involved in anaplerotic reactions, compensating for the depletion of C skeletons consumed by the tricarboxylic acid cycle towards other pathways (synthesis of amino acids) or even other organs (export of malate and citrate via the xylem stream). Part of the phosphoenolpyruvate (PEP) produced by glycolysis may be converted to oxaloacetate and further to malate, with a zero net balance of ATP and NADH during the fixation of two molecules of CO₂. Given the low ARQ values observed here, the resulting malate may not be locally oxidized, but further metabolized to produce, for example, citrate or amino acids. Evidence shows that malate concentration increases in the stem of *Acer platanoides* trees moving upwards (Schill et al., 1996). Transported malate can increase

the malate pool in leaves (Gessler et al., 2009), where it could be metabolized via malic enzymes releasing CO₂, thus favouring carboxylation via Rubisco (Hibberd and Quick 2002). Alternatively, the products can be transported downwards via the phloem (Hoffland et al., 1992; Shane et al., 2004; Touraine et al., 1992), followed by excretion in the rhizosphere as root exudates. Alternatively or additionally, PEPC could be involved in pH regulation (Caburatan & Park, 2021), the latter having appeared stable despite fluctuations in xylem CO₂ (see e.g. Erda et al., 2014). Extrapolating PEPC capacity on a volume basis for comparison with CO₂ efflux or O₂ influx (as in Figure 4) resulted in unrealistically high rates of PEPC fixation (up to two orders of magnitude higher than R_S estimates). First, enzyme activity measured in vitro under saturating substrate usually exceeds the in vivo flux (Junker et al., 2007). Second, PEPC capacity likely decreases with xylem depth (Höll, 1974), and PEPC samples were uniquely taken from the outermost stem tissues. Nevertheless, the high values of PEPC capacity on a volume basis suggest that even low PEPC capacity could be significant for the stem C budget and could help explain the discrepancy between CO₂ efflux and O₂ influx.

4.3 | Other potential C sinks

Another potential missing C sink in R_S budgets is the CO₂ photosynthetic refixation occurring in chloroplast-containing cells located in peripheral woody tissues (Ávila et al., 2014; De Roo et al., 2020; R. O. Teskey et al., 2008), which can reduce stem CO₂ emissions by half, as observed in young poplar trees (De Roo et al., 2020). However, local photosynthetic fixation can be safely discarded within our experimental set-up, as opaque stem chambers were used to measure CO₂ efflux, precluding photosynthetic light reactions. Nevertheless, we cannot discard the possibility of axial diffusion of CO₂ in the gas phase ascribed to distant woody tissue photosynthesis (De Roo et al., 2019; Saveyn, Steppe, & Lemeur, 2008). In this line, light-driven photosynthesis above and below the (opaque) stem chamber can develop light-induced vertical [CO₂] gradients, leading to CO₂ axial diffusion in the gas phase that has been observed to reduce CO₂ efflux by 22% in oak stems (De Roo et al., 2019). Furthermore, we cannot rule out the possibility of O₂ influx measurements overestimating stem respiratory activity. We must critically note that O₂ influx measurements should be considered as additional information that helps disentangle CO₂ sinks and sources, but not as an equivalent to R_S as uncertainties remain. First, a shift in the respiratory substrate from NSCs to lipids or proteins, with a lower oxidation state, requires a higher amount of O₂ for respiratory reduction, hence increasing the ARD (and reducing the ARQ; Fischer et al., 2015; Hanf et al., 2015). However, our study extended over 6 weeks during the summer season and measured NSC concentrations at different heights and depths did not indicate a seasonal NSC depletion that would alter the respiratory substrate (Figure 3). Moreover, beech is not known to store lipids (Hoch et al., 2003), further suggesting the limited role of substrate change

on the ARD. Secondly, nonrespiratory O_2 uptake by O_2 -consuming enzymes like oxidases and hydroxylases (Sweetlove et al., 2013) that are not involved in respiratory metabolism may increase O_2 influx while CO_2 efflux remains constant (Kruse & Adams, 2008; O'Leary et al., 2019; Tcherkez et al., 2012). Thirdly, high growth rates related to cell wall deposition, likely occurring at the end of the growing season, may also lead to a nonrespiratory increase in O_2 consumption, as observed in *Pinus radiata* (Kruse & Adams, 2008).

5 | CONCLUSION AND OUTLOOK

Carbon- and oxygen-based methods to estimate R_5 yield inconsistent results when simultaneously applied to the same individuals under the same conditions. We found a consistent ratio between CO_2 efflux and O_2 influx close to 0.7, which cannot be primarily explained by internal fluxes (xylem CO_2 transport and storage) and might be linked to alternative sinks of respired CO_2 (PEPC fixation and axial CO_2 diffusion) and nonrespiratory O_2 consumption. Remarkably, the high PEPC capacity measured here in mature tree stems, comparable with that observed in current-year greener twigs, points towards PEPC-mediated CO_2 fixation as a relevant driver of the systematic mismatch between CO_2 efflux and O_2 influx. We encourage further research combining CO_2 efflux and O_2 influx readings in parallel with measurements of potential respiration and PEPC capacity at different sapwood depths, as this would help to assess the contribution of inner and outer tissues to total R_5 and how they relate to fluxes at the stem surface. Ideally, incorporating O_2 consumption and biochemical-level knowledge (such as PEPC fixation) into plant mechanistic models could help to more accurately estimate R_5 and better constrain larger-scale C models.

ACKNOWLEDGEMENTS

The authors thank Martin Göbel, Edgar Tunsch, Frank Tiedemann, Dietmar Fellert for technical support, Savoyane Lambert, Nadine Hempel, David Herrera Ramírez for field assistance and Iris Kuhlmann, Anett Enke and Christin Leschik for laboratory support. Thanks to Philip Deman for his help in calibrating the xylem [CO_2] probes. We thank Christian Markwitz for soil water content data. JH acknowledges the continuous support of the International Max Planck Research School for Global Biogeochemical Cycles. We thank the administration of the forestry district Heiligenstadt for the opportunity for research in their forest area. Finally, we are also very grateful to Prof. Aubrey and one anonymous reviewer for their valuable comments. Jan Muhr and Alexander Knohl acknowledge funding by the European Research Council under the European Union's Horizon 2020 research and innovation programme (grant agreement no. 682512 - OXYFLUX). Roberto L. Salomón acknowledges funding from the Research Foundation Flanders (FWO) and the Marie Skłodowska-Curie research programme (grant no. 665501). Open Access funding enabled and organized by Projekt DEAL.

CONFLICT OF INTEREST STATEMENT

The authors declare no conflict of interest.

DATA AVAILABILITY STATEMENT

The data that support the findings of this study are available from the corresponding author upon reasonable request.

ORCID

Juliane Helm  <http://orcid.org/0009-0009-5835-8009>

Roberto L. Salomón  <http://orcid.org/0000-0003-2674-1731>

Boaz Hilman  <http://orcid.org/0000-0003-3403-1561>

Kathy Steppe  <http://orcid.org/0000-0001-6252-0704>

Henrik Hartmann  <http://orcid.org/0000-0002-9926-5484>

REFERENCES

- Acosta, M., Pavelka, M., Pokorný, R., Janouš, D. & Marek, M.V. (2008) Seasonal variation in CO_2 efflux of stems and branches of Norway spruce trees. *Annals of Botany*, 101(3), 469–477.
- Angert, A., Muhr, J., Negron Juárez, R., Alegria Muñoz, W., Kraemer, G., Ramirez Santillan, J., Barkan, E., Mazeh, S., Chambers, J.Q. & Trumbore, S.E. (2012) Internal respiration of Amazon tree stems greatly exceeds external CO_2 efflux. *Biogeosciences*, 9(12), 4979–4991.
- Angert, A. & Sherer, Y. (2011) Determining the relationship between tree-stem respiration and CO_2 efflux by $\delta O_2/Ar$ measurements. *Rapid Communications in Mass Spectrometry*, 25(12), 1752–1756.
- Aubrey, D.P., Boyles, J.G., Krysinsky, L.S. & Teskey, R.O. (2011) Spatial and temporal patterns of xylem sap pH derived from stems and twigs of *Populus deltoides* L. *Environmental and Experimental Botany*, 71(3), 376–381.
- Aubrey, D.P. & Teskey, R.O. (2009) Root-derived CO_2 efflux via xylem stream rivals soil CO_2 efflux. *New Phytologist*, 184(1), 35–40.
- Aubrey, D.P. & Teskey, R.O. (2021) Xylem transport of root-derived CO_2 caused a substantial underestimation of belowground respiration during a growing season. *Global Change Biology*, 27, 2991–3000.
- Ávila, E., Herrera, A. & Tezara, W. (2014) Contribution of stem CO_2 fixation to whole-plant carbon balance in nonsucculent species. *Photosynthetica*, 52(1), 3–15.
- Bénard, C. & Gibon, Y. (2016) Measurement of enzyme activities and optimization of continuous and discontinuous assays. *Current Protocols in Plant Biology*, 1(2), 247–262.
- Berveiller, D. & Damesin, C. (2008) Carbon assimilation by tree stems: potential involvement of phosphoenolpyruvate carboxylase. *Trees*, 22(2), 149–157.
- Bloemen, J., McGuire, M.A., Aubrey, D.P., Teskey, R.O. & Steppe, K. (2013) Transport of root-respired CO_2 via the transpiration stream affects aboveground carbon assimilation and CO_2 efflux in trees. *New Phytologist*, 197(2), 555–565.
- Bowman, W.P., Barbour, M.M., Turnbull, M.H., Tissue, D.T., Whitehead, D. & Griffin, K.L. (2005) Sap flow rates and sapwood density are critical factors in within-and between-tree variation in CO_2 efflux from stems of mature *Dacrydium cupressinum* trees. *New Phytologist*, 167(3), 815–828.
- Burgess, S.S., Adams, M.A., Turner, N.C., Beverly, C.R., Ong, C.K., Khan, A.A. et al. (2001) An improved heat pulse method to measure low and reverse rates of sap flow in woody plants. *Tree Physiology*, 21(9), 589–598.
- Caburatan, L. & Park, J. (2021) Differential expression, tissue-specific distribution, and posttranslational controls of phosphoenolpyruvate carboxylase. *Plants*, 10(9), 1887.

- Campioi, M., Malhi, Y., Vicca, S., Luysaert, S., Papale, D., Peñuelas, J. et al. (2016) Evaluating the convergence between eddy-covariance and biometric methods for assessing carbon budgets of forests. *Nature Communications*, 7(1), 1–12.
- Ceschia, É., Damesin, C., Lebaube, S., Pontailler, J.-Y. & Dufrêne, É. (2002) Spatial and seasonal variations in stem respiration of beech trees (*Fagus sylvatica*). *Annals of Forest Science*, 59(8), 801–812.
- Dejours, P. (1981) Control of respiration. *Principles of Comparative Respiratory Physiology*, 28, 185–220.
- De Roo, L., Bloemen, J., Dupon, Y., Salomón, R.L. & Steppe, K. (2019) Axial diffusion of respired CO₂ confounds stem respiration estimates during the dormant season. *Annals of Forest Science*, 76(2), 1–11.
- De Roo, L., Salomón, R.L. & Steppe, K. (2020) Woody tissue photosynthesis reduces stem CO₂ efflux by half and remains unaffected by drought stress in young *Populus tremula* trees. *Plant, Cell & Environment*, 43(4), 981–991.
- De Schepper, V., Van Dusschoten, D., Copini, P., Jahnke, S. & Steppe, K. (2012) MRI links stem water content to stem diameter variations in transpiring trees. *Journal of Experimental Botany*, 63(7), 2645–2653.
- Erda, F.G., Bloemen, J. & Steppe, K. (2014) Quantifying the impact of daily and seasonal variation in sap pH on xylem dissolved inorganic carbon estimates in plum trees. *Plant Biology*, 16(1), 43–48.
- Fan, H., McGuire, M.A. & Teskey, R.O. (2017) Effects of stem size on stem respiration and its flux components in yellow-poplar (*Liriodendron tulipifera* L.) trees. *Tree Physiology*, 37(11), 1536–1545.
- Fischer, S., Hanf, S., Frosch, T., Gleixner, G., Popp, J., Trumbore, S. et al. (2015) *Pinus sylvestris* switches respiration substrates under shading but not during drought. *New Phytologist*, 207(3), 542–550.
- Gartner, B.L., Moore, J.R. & Gardiner, B.A. (2004) Gas in stems: abundance and potential consequences for tree biomechanics. *Tree Physiology*, 24(11), 1239–1250.
- Gessler, A., Tcherkez, G., Karyanto, O., Keitel, C., Ferrio, J.P., Ghashghaie, J. et al. (2009) On the metabolic origin of the carbon isotope composition of CO₂ evolved from darkened light-acclimated leaves in *Ricinus communis*. *New Phytologist*, 181(2), 374–386.
- Goldstein, G., Andrade, J., Meinzer, F., Holbrook, N., Cavelier, J., Jackson, P. et al. (1998) Stem water storage and diurnal patterns of water use in tropical forest canopy trees. *Plant, Cell & Environment*, 21(4), 397–406.
- Hanf, S., Fischer, S., Hartmann, H., Keiner, R., Trumbore, S., Popp, J. et al. (2015) Online investigation of respiratory quotients in *Pinus sylvestris* and *Picea abies* during drought and shading by means of cavity-enhanced Raman multi-gas spectrometry. *Analyst*, 140(13), 4473–4481.
- Helm, J., Hartmann, H., Göbel, M., Hilman, B., Herrera, D.A. & Muhr, J. (2021) Low-cost chamber design for simultaneous CO₂ and O₂ flux measurements between tree stems and the atmosphere. *Tree Physiology*, 41(9), 1767–1780.
- Hibberd, J.M. & Quick, W.P. (2002) Characteristics of C4 photosynthesis in stems and petioles of C3 flowering plants. *Nature*, 415(6870), 451–454.
- Hilman, B. & Angert, A. (2016) Measuring the ratio of CO₂ efflux to O₂ influx in tree stem respiration. *Tree Physiology*, 36(11), 1422–1431.
- Hilman, B., Muhr, J., Trumbore, S.E., Kunert, N., Carbone, M.S., Yuval, P. et al. (2019) Comparison of CO₂ and O₂ fluxes demonstrate retention of respired CO₂ in tree stems from a range of tree species. *Biogeosciences*, 16(1), 177–191.
- Hoch, G., Richter, A. & Körner, C. (2003) Non-structural carbon compounds in temperate forest trees. *Plant, Cell & Environment*, 26(7), 1067–1081.
- Hoffland, E., van den Boogaard, R., Nelemans, J. & Findenegg, G. (1992) Biosynthesis and root exudation of citric and malic acids in phosphate-starved rape plants. *New Phytologist*, 122(4), 675–680.
- Höll, W. (1974) Dark CO₂ fixation by cell-free preparations of the wood of *Robinia pseudoacacia*. *Canadian Journal of Botany*, 52(4), 727–734.
- Ivanov, A.G., Krol, M., Sveshnikov, D., Malmberg, G., Gardeström, P., Hurry, V. et al. (2006) Characterization of the photosynthetic apparatus in cortical bark chlorenchyma of Scots pine. *Planta*, 223, 1165–1177.
- Junker, B.H., Lonien, J., Heady, L.E., Rogers, A. & Schwender, J. (2007) Parallel determination of enzyme activities and in vivo fluxes in *Brassica napus* embryos grown on organic or inorganic nitrogen source. *Phytochemistry*, 68(16–18), 2232–2242.
- Kruse, J. & Adams, M.A. (2008) Integrating two physiological approaches helps relate respiration to growth of *Pinus radiata*. *New Phytologist*, 180(4), 841–852.
- Landhäusser, S.M., Chow, P.S., Dickman, L.T., Furze, M.E., Kuhlman, I., Schmid, S. et al. (2018) Standardized protocols and procedures can precisely and accurately quantify non-structural carbohydrates. *Tree Physiology*, 38(12), 1764–1778.
- Lavigne, M., Franklin, S., Hunt, Jr. E. (1996) Estimating stem maintenance respiration rates of dissimilar balsam fir stands. *Tree Physiology*, 16(8), 687–695.
- Levy, P., Meir, P., Allen, S. & Jarvis, P. (1999) The effect of aqueous transport of CO₂ in xylem sap on gas exchange in woody plants. *Tree Physiology*, 19(1), 53–58.
- Maier, C.A., Johnsen, K.H., Clinton, B.D. & Ludovici, K.H. (2010) Relationships between stem CO₂ efflux, substrate supply, and growth in young loblolly pine trees. *New Phytologist*, 185(2), 502–513.
- Masiello, C., Gallagher, M., Randerson, J., Deco, R. & Chadwick, O. (2008) Evaluating two experimental approaches for measuring ecosystem carbon oxidation state and oxidative ratio. *Journal of Geophysical Research: Biogeosciences*, 113, G03010.
- McGuire, M., Cerasoli, S. & Teskey, R. (2007) CO₂ fluxes and respiration of branch segments of sycamore (*Platanus occidentalis* L.) examined at different sap velocities, branch diameters, and temperatures. *Journal of Experimental Botany*, 58(8), 2159–2168.
- McGuire, M. & Teskey, R. (2002) Microelectrode technique for in situ measurement of carbon dioxide concentrations in xylem sap of trees. *Tree Physiology*, 22(11), 807–811.
- McGuire, M. & Teskey, R. (2004) Estimating stem respiration in trees by a mass balance approach that accounts for internal and external fluxes of CO₂. *Tree Physiology*, 24(5), 571–578.
- Nakagawa, S. & Schielzeth, H. (2013) A general and simple method for obtaining R² from generalized linear mixed-effects models. *Methods in ecology and evolution*, 4(2), 133–142.
- Nobel, P.S. (2009) *Physicochemical & environmental plant physiology*, 4th edition. Academic Press.
- O'Leary, B.M., Asao, S., Millar, A.H. & Atkin, O.K. (2019) Core principles which explain variation in respiration across biological scales. *New Phytologist*, 222(2), 670–686.
- Pfanz, H., Aschan, G., Langenfeld-Heyser, R., Wittmann, C. & Loose, M. (2002) Ecology and ecophysiology of tree stems: cortical and wood photosynthesis. *Naturwissenschaften*, 89(4), 147–162.
- Pinheiro, J., Bates, D., DebRoy, S., Sarkar, D. & Van Heisterkamp, S. et al. (2017) *Package 'nlme'*. Linear and nonlinear mixed effects models, version 3.1–96.
- R Development Core Team. 2019. *R: A language and environment for statistical computing*. R Foundation for Statistical Computing.
- Rodríguez-Calcerrada, J., Martin-StPaul, N.K., Lempereur, M., Ourcival, J.-M., del Rey, M.d.C., Joffre, R. et al. (2014) Stem CO₂ efflux and its contribution to ecosystem CO₂ efflux decrease with drought in a Mediterranean forest stand. *Agricultural and Forest Meteorology*, 195, 61–72.
- Ryan, M.G., Gower, S.T., Hubbard, R.M., Waring, R.H., Gholz, H.L., Cropper, W.P. et al. (1995) Woody tissue maintenance respiration of four conifers in contrasting climates. *Oecologia*, 101(2), 133–140.
- Salomón, R.L., Rodríguez-Calcerrada, J. & Staudt, M. (2017) Carbon losses from respiration and emission of volatile organic compounds—the

- overlooked side of tree carbon budgets. In: Gil-Pelegrín, E., Peguero-Pina, J. & Sancho-Knapik, D. (Eds.) *Oaks Physiological Ecology. Exploring the Functional Diversity of Genus Quercus L.*, Tree Physiology, 7. Springer, pp. 327–359.
- Salomón, R.L., De Schepper, V., Valbuena-Carabaña, M., Gil, L. & Steppe, K. (2018) Daytime depression in temperature-normalised stem CO₂ efflux in young poplar trees is dominated by low turgor pressure rather than by internal transport of respired CO₂. *New Phytologist*, 217(2), 586–598.
- Salomón, R., Valbuena-Carabaña, M., Teskey, R., McGuire, M.A., Aubrey, D., González-Doncel, I. et al. (2016) Seasonal and diel variation in xylem CO₂ concentration and sap pH in sub-Mediterranean oak stems. *Journal of Experimental Botany*, 67(9), 2817–2827.
- Saveyn, A., Steppe, K. & Lemeur, R. (2008) Report on non-temperature related variations in CO₂ efflux rates from young tree stems in the dormant season. *Trees*, 22(2), 165–174.
- Saveyn, A., Steppe, K., McGuire, M.A., Lemeur, R. & Teskey, R.O. (2008) Stem respiration and carbon dioxide efflux of young *Populus deltoides* trees in relation to temperature and xylem carbon dioxide concentration. *Oecologia*, 154(4), 637–649.
- Schill, V., Hartung, W., Orthen, B. & Weisenseel, M.H. (1996) The xylem sap of maple (*Acer platanoides*) trees - sap obtained by a novel method shows changes with season and height. *Journal of Experimental Botany*, 47, 123–133.
- Shane, M.W., Cramer, M.D., Funayama-Noguchi, S., Cawthray, G.R., Millar, A.H., Day, D.A. et al. (2004) Developmental physiology of cluster-root carboxylate synthesis and exudation in harsh hakea. Expression of phospho enol pyruvate carboxylase and the alternative oxidase. *Plant Physiology*, 135(1), 549–560.
- Steppe, K., De Pauw, D.J., Doody, T.M. & Teskey, R.O. (2010) A comparison of sap flux density using thermal dissipation, heat pulse velocity and heat field deformation methods. *Agricultural and Forest Meteorology*, 150(7–8), 1046–1056.
- Steppe, K., Saveyn, A., McGuire, M.A., Lemeur, R. & Teskey, R.O. (2007) Resistance to radial CO₂ diffusion contributes to between-tree variation in CO₂ efflux of *Populus deltoides* stems. *Functional Plant Biology*, 34(9), 785–792.
- Steppe, K., Sterck, F. & Deslauriers, A. (2015) Diel growth dynamics in tree stems: linking anatomy and ecophysiology. *Trends in Plant Science*, 20(6), 335–343.
- Sweetlove, L.J., Williams, T.C., Cheung, C.M. & Ratcliffe, R.G. (2013) Modelling metabolic CO₂ evolution—a fresh perspective on respiration. *Plant, Cell & Environment*, 36(9), 1631–1640.
- Tamrakar, R., Rayment, M.B., Moyano, F., Mund, M. & Knohl, A. (2018) Implications of structural diversity for seasonal and annual carbon dioxide fluxes in two temperate deciduous forests. *Agricultural and Forest Meteorology*, 263, 465–476.
- Tarvainen, L., Henriksson, N., Näsholm, T. & Marshall, J.D. (2023) Among-species variation in sap pH affects the xylem CO₂ transport potential in trees. *New Phytologist*, 238(3), 926–931.
- Tcherkez, G., Boex-Fontvieille, E., Mahé, A. & Hodges, M. (2012) Respiratory carbon fluxes in leaves. *Current Opinion in Plant Biology*, 15(3), 308–314.
- Teskey, R. & McGuire, M. (2007) Measurement of stem respiration of sycamore (*Platanus occidentalis* L.) trees involves internal and external fluxes of CO₂ and possible transport of CO₂ from roots. *Plant, Cell & Environment*, 30(5), 570–579.
- Teskey, R.O., Saveyn, A., Steppe, K. & McGuire, M.A. (2008) Origin, fate and significance of CO₂ in tree stems. *New Phytologist*, 177(1), 17–32.
- Touraine, B., Muller, B. & Grignon, C. (1992) Effect of phloem-translocated malate on NO₃⁻ uptake by roots of intact soybean plants. *Plant Physiology*, 99(3), 1118–1123.
- Trumbore, S.E., Angert, A., Kunert, N., Muhr, J. & Chambers, J.Q. (2013) What's the flux? Unraveling how CO₂ fluxes from trees reflect underlying physiological processes. *New Phytologist*, 197(2), 353–355.
- Yang, J., He, Y., Aubrey, D.P., Zhuang, Q. & Teskey, R.O. (2016) Global patterns and predictors of stem CO₂ efflux in forest ecosystems. *Global Change Biology*, 22(4), 1433–1444.

SUPPORTING INFORMATION

Additional supporting information can be found online in the Supporting Information section at the end of this article.

How to cite this article: Helm, J., Salomón, R.L., Hilman, B., Muhr, J., Knohl, A., Steppe, K. et al. (2023) Differences between tree stem CO₂ efflux and O₂ influx rates cannot be explained by internal CO₂ transport or storage in large beech trees. *Plant, Cell & Environment*, 1–14.

<https://doi.org/10.1111/pce.14614>